

## Novel Fluorescent Cationic Silver Thiosemicarbazone Clusters Containing Different Eight-Membered Ag<sub>4</sub>S<sub>4</sub> Metallacycles

Alfonso Castiñeiras and Rosa Pedrido\*

Departamento de Química Inorgánica, Facultad de Farmacia, Universidade de Santiago de Compostela, Santiago de Compostela, 15782 Spain

Received January 13, 2009

The reaction of silver acetate and silver nitrate with the new phosphinethiosemicarbazone ligand 2-(2-(diphenylphosphino)benzylidene)-N-ethylthiosemicarbazone (HLPEt) gave rise to the complexes [Ag(LPEt)]<sub>4</sub>·2MeOH (**1**) and [Ag<sub>2</sub>(LPEt)(HLPEt)]<sub>2</sub>·(NO<sub>3</sub>)<sub>2</sub> (**3**). Slow crystallization of the mother liquors obtained from the synthesis of **1** and **3** afforded suitable crystals of [Ag<sub>2</sub>(LPEt)(HLPEt)]<sub>2</sub>(CH<sub>3</sub>COO)<sub>2</sub>·6MeOH (**2**) and [Ag<sub>2</sub>(LPEt)(HLPEt)]<sub>2</sub>(NO<sub>3</sub>)<sub>2</sub>·2MeOH·2H<sub>2</sub>O (**4**), respectively. Complexes **2** and **4** are tetranuclear silver clusters displaying a similar Ag<sub>4</sub>S<sub>4</sub>P<sub>4</sub> core, but containing different sizes, conformations for the Ag<sub>4</sub>S<sub>4</sub> metallacycles, and crystal packings. The four complexes are strongly luminescent in methanol solutions. A comparison between the emission bands of compounds **1**–**4** lead us to conclude that the luminescence is notably affected by the charge and the counterion of the cluster.

### Introduction

Metal-induced self-assembly is an active area of study in the field of host–guest and supramolecular chemistry.<sup>1</sup> Fujita et al.<sup>2</sup> and Stang et al.<sup>3</sup> have shown that well-defined structures such as macrocycles, cages, and catenanes can be obtained by mixing the appropriate building blocks. The incorporation of flexible components with suitable geometrical preferences in molecular architectures can lead to the formation of discrete structures that range from simple squares, through higher polygons, to larger polyhedrons. The formation of this type of assembled species has attracted specific attention, as there has been considerable progress toward the application of such materials in molecular recognition, enantioselective sensing, photoluminescence, and catalysis.<sup>3,4</sup>

Particularly, in the area of the metal-containing polygons, those incorporating Ag<sub>x</sub>S<sub>x</sub> cycles (x = 2, 3, 4) are among the less-studied structures. Thus, the few reported examples

showing a Ag<sub>4</sub>S<sub>4</sub> central ring were assembled from simple mercapto-derivates,<sup>5</sup> thiocyanates,<sup>6</sup> thioether macrocycles,<sup>7</sup> or sulfanyl carboxylate ligands.<sup>8</sup>

On the other hand, a great deal of work has been devoted to the study of polydentate thiosemicarbazones because of their probed versatility as ligands, which arises from the variety in number and nature of their donor atoms.<sup>9</sup> In particular, thiosemicarbazone ligands in combination with the various coordination geometries of Ag(I) ions give rise to discrete molecular architectures of polyhedral or polygonal shapes and infinite coordination polymers. Nevertheless, these silver thiosemicarbazone complexes are usually stabilized by phosphine as coligands.<sup>10</sup> The number of silver complexes exclusively derived from thiosemicarbazones is still very low, probably due to insolubility or polymerization problems. The few reported cases of homoleptic thiosemicarbazone complexes consist of tetranuclear or hexanuclear

\*To whom correspondence should be addressed. Fax: +34 981 597 525. E-mail: rosa.pedrido@usc.es.

(1) Khlbystov, A. N.; Blake, A. J.; Champness, N. R.; Lemenovskii, D. A.; Majouga, A. G.; Zyk, N. V.; Schröder, M. *Coord. Chem. Rev.* **2001**, *222*, 155–192. Batten, S. R.; Robson, R. *Angew. Chem., Int. Ed.* **1998**, *37*, 1461–1494.

(2) Fujita, M. *Chem. Soc. Rev.* **1998**, *27*, 417–425.  
(3) Stang, P. J.; Cao, D. H.; Saito, S.; Arif, A. M. *J. Am. Chem. Soc.* **1984**, *106*, 258–264. Stang, P. J.; Cao, D. H. *J. Am. Chem. Soc.* **1994**, *116*, 4981–4982. Leininger, S.; Olenyuk, B.; Stang, P. J. *Chem. Rev.* **2000**, *100*, 853–908. Seidel, S. R.; Stang, P. J. *Acc. Chem. Res.* **2002**, *35*, 972–983. Northrop, B. H.; Yang, H.-B.; Stang, P. J. *Chem. Commun.* **2008**, 5896–5908.

(4) Würthner, F.; You, C.-C.; Saha-Möller, C. R. *Chem. Soc. Rev.* **2004**, *33*, 133–146. Nishioka, Y.; Yamaguchi, T.; Kawano, M.; Fujita, M. *J. Am. Chem. Soc.* **2008**, *130*, 8160–8161.

(5) Tsyba, I.; Mui, B. B.; Bau, R.; Noguchi, R.; Nomiya, K. *Inorg. Chem.* **2003**, *48*, 8028–8032. Zartilas, S.; Kourkoumelis, N.; Hadjikakou, S. K.; Hadjiliadis, N.; Zachariadis, P.; Kubicki, M.; Denisov, A. Y.; Butler, I. S. *Eur. J. Inorg. Chem.* **2007**, 1219–1224.

(6) Günnes, M.; Valkonen, J. *Acta Crystallogr., Sect. C* **2004**, *C60*, i101–i103.

(7) Jenkins, H. A.; Loeb, S. J.; Malats i Riera, A. *Inorg. Chim. Acta* **1996**, *246*, 207–215. Yamaguchi, T.; Yamazaki, F.; Ito, T. *Acta Crystallogr., Sect. C* **2002**, *C58*, m213–m214.

(8) Deivaraj, T. C.; Vittal, J. J. *J. Chem. Soc., Dalton Trans.* **2001**, 329–335. Barreiro, E.; Casas, J. S.; Couce, M. D.; Sánchez, A.; Seoane, R.; Sordo, J.; Varela, J. M.; Vázquez-López, E. M. *Dalton Trans.* **2007**, 3074–3085.

(9) Casas, J. S.; García-Tasende, M. S.; Sordo, J. *Coord. Chem. Rev.* **2000**, *209*, 197–261.

(10) Lobana, T. S.; Khanna, S.; Sharma, R.; Hundal, G.; Sultana, R.; Chaudhary, M.; Butcher, R. J.; Castiñeiras, A. *Cryst. Growth Des.* **2008**, *8*, 1203–1212.

cluster arrays formed by means of a self-assembly process.<sup>11</sup> A careful study of these clusters let us identify several  $\text{Ag}_x\text{S}_x$  metallacycle examples, although we must stress that none of these silver complexes were described for the authors as metallacycle-containing structures. We have recently published a pair of new  $\text{Ag}_4\text{S}_4\text{P}_4$  clusters,  $[\text{Ag}_4(\text{LPPh})_4]^{\text{a}}[\text{Ag}_4(\text{LPPH})_4]^{\text{b}} \cdot 8\text{MeOH}$ , which feature three consecutive  $\text{Ag}_2\text{S}_2$  metallacycles due to the role of some of the sulfur atoms acting as  $\mu_3$ -bridges.<sup>12</sup> Dilworth et al. reported the  $\text{Ag}_6\text{S}_6\text{N}_6$  hexamer complex  $[\text{Ag}_6(\text{L}^1\text{H})_6] \cdot 6\text{DMF}$  derived from a salicylaldehyde thiosemicarbazone, which exhibits two six-membered  $\text{Ag}_3\text{S}_3$  rings in a chair configuration, stacked one above the other and linked together by six bridging ligands.<sup>13</sup> In 2006, Nomiya et al. published the  $\text{Ag}_4\text{S}_4\text{N}_4$  silver cluster  $[\text{Ag}(\text{mtsc})]_4 \cdot 2\text{CHCl}_3$ , derived from 4-N-morpholeyl 2-acetylpyridine, which features a  $\text{Ag}_4\text{S}_4$  metallacycle example.<sup>14</sup>

As a part of an ongoing research project dealing with the factors involved in the assembly of clusters by exclusively using thiosemicarbazones, we have decided to explore the coordination behavior of a new thiosemicarbazone ligand bearing a phosphine group toward silver (I) ions, but using two different silver sources. The results achieved are reported herein.

## Experimental Section

**Materials.** All solvents, 2-diphenylphosphinobenzaldehyde, 4-N-ethylthiosemicarbazide, silver(I) acetate, silver(I) nitrate, and triphenylphosphine are commercially available and were used without further purification.

**Methods.** Elemental analyses of C, H, N, and S were performed on a FISON EA 1108 analyzer.  $^1\text{H}$ ,  $^{13}\text{C}$ , and  $^{31}\text{P}$  NMR studies ( $\text{H}_3\text{PO}_4$  was used as an internal reference) were performed in a VARIAN MERCURY 300 spectrometer. Infrared spectra were measured from KBr pellets on a BRUKER IFS-66V spectrophotometer in the ranges 4000–400 and 500–100  $\text{cm}^{-1}$ . Electrospray ionization mass spectra (ESI) were recorded on an API4000 Applied Biosystems mass spectrometer with a Triple Quadrupole analyzer. Conductivity was measured at 25 °C from  $10^{-3}$  M solutions in DMF on a Crison micro CM 2200 conductivitymeter. UV data were measured in a Hewlett-Packard 8452A. Luminescence was recorded in a Jovin Yvon-Spex Fluoromax-2 spectrophotometer.

**Ligand Synthesis.** The ligand 2-(2-(diphenylphosphino)benzylidene)-N-ethylthiosemicarbazone (HLPet) was prepared by equimolecular condensation of 2-diphenylphosphinobenzaldehyde and 4-N-ethyl-3-thiosemicarbazide. The experimental procedure and characterization details are shown below.

Over a solution of 2-diphenylphosphinobenzaldehyde (0.5 g, 1.7 mmol) in ethanol was added 4-N-ethyl-3-thiosemicarbazide (0.21 g, 1.7 mmol). The solution was heated under reflux over a 3 h period, then concentrated to ca. 5  $\text{cm}^3$  and cooled overnight (4 °C). The soft yellow crystalline precipitate was filtered off, washed with diethyl ether ( $3 \times 5$  mL), and dried in vacuo.

**HLPet.** Yield 90%; mp = 198 °C. Elem anal. found: C, 67.5; H, 5.8; N, 10.6; S, 8.2.  $\text{C}_{22}\text{H}_{22}\text{N}_3\text{P}_1\text{S}_1$  calcd: C, 67.5; H, 5.7; N, 10.7; S, 8.2.  $\text{ES}^+$ : 392.1  $[\text{HLPet} + \text{H}]^+$ .  $^1\text{H}$  NMR (DMSO- $d_6$ , ppm):  $\delta$  1.08 (t, 3H), 3.50 (q, 2H), 6.77 (m, 1H), 7.19

(m, 4H), 7.41 (m, 8H), 8.19 (s, 2H), 8.65 (bs, 1H), 11.58 (s, 1H).  $^{13}\text{C}$  NMR (DMSO- $d_6$ , ppm):  $\delta$  176.74 (C=S), 140.35 (C=N), 137.97–127.44 ( $\text{C}_{\text{ar}}$ ), 38.88 ( $\text{CH}_2$ ), 14.74 ( $\text{CH}_3$ ).  $^{31}\text{P}$  NMR (DMSO- $d_6$ , ppm):  $\delta$  -10.82. IR (KBr,  $\text{cm}^{-1}$ ):  $\nu(\text{NH})$  3364, 3343,  $\nu(\text{C}=\text{N}) + \nu(\text{C}-\text{N})$  1583, 1530, 1434,  $\nu(\text{C}=\text{S})$  749,  $\nu(\text{N}-\text{N})$  1099. UV/vis (nm): 330, 290, 325.

**Preparation of the Complexes.** Complexes **1** and **3** were obtained by chemical synthesis, using silver(I) acetate and silver (I) nitrate as metal precursors. Crystallization of the reaction solutions afforded crystals of **2** and **4**, respectively. The procedures followed are detailed below.

**$[\text{Ag}(\text{LPet})]_4 \cdot 2\text{MeOH}$ , **1**.** A total of 0.021 g (0.13 mmol) of silver(I) acetate was added over the ligand HLPet (0.05 g, 0.13 mmol), previously dissolved in methanol (50 mL). The deep yellow solution formed was refluxed for 3 h and then left stirring overnight. After that time, the solution was concentrated until a small volume (20 mL) was reached, and the suspended yellow solid was filtered out, washed with diethyl ether, and finally dried in vacuo.

**$[\text{Ag}(\text{LPPH})]_4 \cdot 2\text{MeOH}$ , **1**.** Yield 89%. Elem anal. found: C, 52.6; H, 4.4; N, 8.2; S, 6.1.  $\text{Ag}_4\text{C}_{90}\text{H}_{92}\text{N}_{12}\text{O}_2\text{P}_4\text{S}_4$  calcd: C, 52.5; H, 4.5; N, 8.2; S, 6.2.  $\text{ES}^+$ : 499.1  $[\text{AgL} + \text{H}]^+$ ; 997.6  $[\text{Ag}_2\text{L}_2 + \text{H}]^+$ ; 1105.5  $[\text{Ag}_3\text{L}_2 + \text{H}]^+$ ; 1994.2  $[\text{Ag}_4\text{L}_4 + \text{H}]^+$ .  $^1\text{H}$  NMR (DMSO- $d_6$ , ppm): 1.87 (t, 3H), 2.50 (m, 2H +  $\text{H}_2\text{O}$ ); 6.70–7.84 (m, 15H), 8.43 (s, 1H).  $^{31}\text{P}$  NMR (DMSO- $d_6$ , ppm): 7.91. IR (KBr,  $\text{cm}^{-1}$ ):  $\nu(\text{OH}) + \nu(\text{NH})$  3431,  $\nu(\text{C}=\text{N}) + \nu(\text{C}-\text{N})$  1555, 1517,  $\nu(\text{N}-\text{N})$  1094,  $\nu(\text{C}=\text{S})$  799. UV/vis (nm):  $\lambda$  220, 280, 350.  $\Lambda_{\text{M}} = 46.0 \text{ S m}^2 \text{ mol}^{-1}$ .

Slow crystallization of the mother liquors led to the isolation of yellow prism crystals of a different complex,  $[\text{Ag}_2(\text{LPet})(\text{HLPet})]_2(\text{AcO})_2 \cdot 6\text{MeOH}$  (**2**), which was completely characterized, including X-ray diffraction.

**$[\text{Ag}_2(\text{LPet})(\text{HLPet})]_2(\text{AcO})_2 \cdot 6\text{MeOH}$ , **2**.** Yield 6%. Elem anal. found: C, 51.1; H, 5.0; N, 7.4; S, 5.7.  $\text{Ag}_4\text{C}_{98}\text{H}_{116}\text{N}_{12}\text{O}_{10}\text{P}_4\text{S}_4$  calcd: C, 51.0; H, 5.1; N, 7.3; S, 5.6.  $\text{ES}^+$ : 499.9  $[\text{Ag}(\text{HL}) + \text{H}]^+$ ; 998.4  $[\text{Ag}_2(\text{L})(\text{HL}) + \text{H}]^+$ ; 1497.0  $[\text{Ag}_3(\text{HL})_2(\text{L}) + \text{H}]^+$ .  $^1\text{H}$  NMR (DMSO- $d_6$ , ppm): 1.87 (t, 3H), 2.50 (m, 2H +  $\text{H}_2\text{O}$ ); 6.72–7.82 (m, 15H), 8.42 (s, 1H), 11.62 (s, 1H).  $^{31}\text{P}$  NMR (DMSO- $d_6$ , ppm): 8.83; IR (KBr,  $\text{cm}^{-1}$ ):  $\nu(\text{OH}) + \nu(\text{NH})$  3418, 3343,  $\nu(\text{C}=\text{N}) + \nu(\text{C}-\text{N})$  1555, 1517,  $\nu(\text{N}-\text{N})$  1095,  $\nu(\text{C}=\text{S})$  799,  $\nu_{\text{as}}(\text{COO})$  1579,  $\nu_{\text{s}}(\text{COO})$  1435. UV/vis (nm):  $\lambda$  220, 280, 350.  $\Lambda_{\text{M}} = 79.3 \text{ S m}^2 \text{ mol}^{-1}$ .

**$[\text{Ag}_2(\text{LPet})(\text{HLPet})]_2 \cdot (\text{NO}_3)_2$ , **3**.** A total of 0.022 g (0.13 mmol) of silver(I) nitrate was added over the ligand HLPet (0.05 g, 0.13 mmol), previously dissolved in methanol (50 mL). The soft yellow solution formed was refluxed for 3 h and then left stirring overnight. After that, the solution was concentrated until a small volume (20 mL) was reached, and the soft yellow suspended solid was filtered out, washed with diethyl ether, and finally dried in vacuo.

**$[\text{Ag}_2(\text{LPet})(\text{HLPet})]_2(\text{NO}_3)_2$ , **3**.** Yield 54%. Elem anal. found: C, 49.6; H, 4.2; N, 9.4; S, 5.9.  $\text{Ag}_4\text{C}_{88}\text{H}_{88}\text{N}_{14}\text{O}_6\text{P}_4\text{S}_4$  calcd: C, 49.8; H, 4.2; N, 9.2; S, 6.0.  $\text{ES}^+$ : 499.9  $[\text{Ag}(\text{HL}) + \text{H}]^+$ ; 998.4  $[\text{Ag}_2(\text{L})(\text{HL}) + \text{H}]^+$ ; 1497.1  $[\text{Ag}_3(\text{HL})_2(\text{L}) + \text{H}]^+$ .  $^1\text{H}$  NMR (DMSO- $d_6$ , ppm): 1.05 (t, 12H), 3.30 (m, 8H +  $\text{H}_2\text{O}$ ), 6.74 (m, 8H); 7.39 (m, 24H), 7.53 (m, 16H), 7.75 (m, 8H), 8.02 (bs, 2H), 8.29 (bs, 2H), 8.46(s, 2H), 9.04 (bs, 2H), 11.48 (s, 1H), 11.67 (s, 1H).  $^{31}\text{P}$  NMR (DMSO- $d_6$ , ppm): 8.8. IR (KBr,  $\text{cm}^{-1}$ ):  $\nu(\text{OH}) + \nu(\text{NH})$  3431, 3229,  $\nu(\text{C}=\text{N}) + \nu(\text{C}-\text{N})$  1583, 1555,  $\nu(\text{N}-\text{N})$  1096,  $\nu(\text{C}=\text{S})$  801,  $\nu(\text{NO}_3)$  1384 vs and 1293 s. UV/vis (nm):  $\lambda$  220, 280, 320, 350.  $\Lambda_{\text{M}} = 66.1 \text{ S m}^2 \text{ mol}^{-1}$ .

Slow crystallization of the mother liquors led to the isolation of yellow crystals of the complex  $[\text{Ag}_2(\text{LPet})(\text{HLPet})]_2(\text{NO}_3)_2 \cdot 2\text{MeOH}$  (**4**), which was also completely characterized, including its crystal structure.

**$[\text{Ag}_2(\text{LPet})(\text{HLPet})]_2(\text{NO}_3)_2 \cdot 2\text{MeOH} \cdot 2\text{H}_2\text{O}$ , **4**.** Yield: 25%. Elem anal. found: C, 49.4; H, 4.3; N, 8.7; S, 5.9.  $\text{Ag}_4\text{C}_{90}\text{H}_{96}\text{N}_{14}\text{O}_8\text{P}_4\text{S}_4$  calcd: C, 49.5; H, 4.4; N, 8.9; S, 5.9.  $\text{ES}^+$ : 499.9  $[\text{Ag}(\text{HL}) + \text{H}]^+$ ; 998.4  $[\text{Ag}_2(\text{L})(\text{HL}) + \text{H}]^+$ ; 1497.0

(11) Bermejo, M. R.; González-Noya, A. M.; Pedrido, R. M.; Romero, M. J.; Vázquez, M. *Angew. Chem., Int. Ed.* **2005**, *117*, 4254–4259. Bermejo, M. R.; González-Noya, A. M.; Martínez-Calvo, M.; Pedrido, R.; Romero, M. J.; Vázquez López, M. *Eur. J. Inorg. Chem.* **2008**, *24*, 3852–3863.

(12) Castiñeiras, A.; Pedrido, R. *Inorg. Chem.* **2008**, *47*, 5534–5536.

(13) Ashfield, L. J.; Cowley, A. R.; Dilworth, J. R.; Donnelly, P. S. *Inorg. Chem.* **2004**, *43*, 4121–4123.

(14) Onodera, K.; Kasuga, N. C.; Takashima, T.; Hara, A.; Amano, A.; Murakami, H.; Nomiya, K. *Dalton Trans* **2007**, 3646–3652.

[Ag<sub>3</sub>(HL)<sub>2</sub>(L) + H]<sup>+</sup>. <sup>1</sup>H NMR (DMSO-d<sub>6</sub>, ppm): 1.05 (t, 12H), 3.48 (m, 8H), 6.74 (m, 8H); 7.39 (m, 24H), 7.53 (m, 16H), 7.75 (m, 8H), 8.02 (bs, 2H), 8.29 (bs, 2H), 8.46 (s, 2H), 9.04 (bs, 2H), 11.48 (s, 1H), 11.67 (s, 1H). <sup>31</sup>P NMR (DMSO-d<sub>6</sub>, ppm): 9.2, 11.2. IR (KBr, cm<sup>-1</sup>): ν(OH) + ν(NH) 3431, 3228, ν(C=N) + ν(C-N) 1584, 1555, ν(N-N) 1096, ν(C=S) 801, ν(NO<sub>3</sub>) 1384. UV/vis (nm): λ 220, 280, 320, 350. Λ<sub>M</sub> = 69.3 S m<sup>2</sup> mol<sup>-1</sup>.

**Crystal Structure Determinations.** Colorless needle and prismatic crystals of **2** and **4**, respectively, were mounted on a glass fiber and used for data collection. Crystal data were collected at 100(2) K, using a Bruker X8 Kappa APEXII diffractometer. Graphite monochromated MoK(α) radiation (λ = 0.71073 Å) was used throughout. The data were processed with APEX2<sup>15</sup> and corrected for absorption using SADABS.<sup>16</sup> The structure was solved by direct methods using the program SHELXS-97<sup>17</sup> and refined by full-matrix least-squares techniques against F<sup>2</sup> using SHELXL-97.<sup>17</sup> Positional and anisotropic atomic displacement parameters were refined for all heteroatoms. Hydrogen atoms bonded to carbon were placed geometrically. The O–H and N–H hydrogen atoms were initially positioned at sites determined from difference maps, but the positional parameters for all H atoms were included as fixed contributions riding on attached atoms with isotropic thermal parameters 1.2 times those of their carrier atoms. Criteria of a satisfactory complete analysis were ratios of “rms” shift to standard deviation of less than 0.001 and no significant features in the final difference maps. Molecular graphics came from DIAMOND.<sup>18</sup> A summary of the crystal data, experimental details, and refinement results are listed in Table 1. Significant bond distances and angles are summarized in Table 2, while hydrogen bond interaction parameters are listed in Table 3.

CCDC 713941 and 713942 contain the supplementary crystallographic data for this paper. These data can be obtained free of charge from the Cambridge Crystallographic Data Centre via www.ccdc.cam.ac.uk/data\_request.cif.

## Results and Discussion

**Synthesis and Characterization.** The phosphino thiosemicarbazone ligand 2-(2-(diphenylphosphino)benzylidene)-N-ethylthiosemicarbazone (HLPEt, Scheme 1) was prepared by the 1:1 molar reaction of 2-diphenylphosphinobenzaldehyde and 4-N-ethyl-3-thiosemicarbazide. Reaction of the isolated HLPEt with silver(I) acetate resulted in the formation of a deep yellow solution, which after partial concentration gave rise to the solid tetranuclear compound [Ag(LPEt)]<sub>4</sub>·2MeOH (**1**). Slow evaporation of the mother liquors afforded suitable crystals corresponding to [Ag<sub>2</sub>(LPEt)(HLPEt)]<sub>2</sub>(AcO)<sub>2</sub>·6MeOH (**2**). The stoichiometry shown by the cationic crystalline compound **2** was unexpected because two of the four ligands have experienced a protonation process during the crystallization. Normally, acetate metal salts are basic enough to deprotonate the thiosemicarbazone ligands, and therefore, the stoichiometry of the isolated solid and that of the crystallized compound used to be similar.<sup>12</sup>

When the ligand HLPEt was reacted with silver nitrate, we obtained the powdery complex [Ag<sub>2</sub>(LPEt)(HLPEt)]<sub>2</sub>(NO<sub>3</sub>)<sub>2</sub>·2MeOH (**3**), after partial removal of the solvent. In this case, a slow evaporation of the mother liquors gave

**Table 1.** Crystal Data and Structure Refinement for Compounds **2** and **4**

	<b>2</b>	<b>4</b>
empirical formula	C <sub>98</sub> H <sub>116</sub> Ag <sub>4</sub> N <sub>12</sub> O <sub>10</sub> P <sub>4</sub> S <sub>4</sub>	C <sub>90</sub> H <sub>98</sub> Ag <sub>4</sub> N <sub>14</sub> O <sub>10</sub> P <sub>4</sub> S <sub>4</sub>
fw	2305.63	2219.42
cryst syst	triclinic	triclinic
temp (K)	100(2)	100(2)
space group	P $\bar{1}$	P $\bar{1}$
unit cell dimensions		
a/Å	13.2286(9)	13.4372(11)
b/Å	14.8548(9)	13.8690(11)
c/Å	15.6936(16)	14.9520(10)
α/deg	107.758(5)	103.724(3)
β/deg	107.242(5)	102.773(3)
γ/deg	107.849(4)	96.866(3)
Volume/Å <sup>-3</sup>	2523.8(3)	2596.1(3)
Z	1	1
calcd density/Mg/m <sup>3</sup>	1.517	1.420
abs. coeff./mm <sup>-1</sup>	0.973	0.944
F(000)	1180	1128
cryst size	0.19 × 0.09 × 0.08	0.07 × 0.06 × 0.06
θ range/deg	1.51–25.68	1.45–23.33
Limiting indices/h, k, l	−16/15, −18/17, 0/19	−14/14, −15/14, 0/16
reflns collect/unique (R <sub>int</sub> )	57185/9520 (0.0563)	31927/7466 (0.0569)
completeness θ/° (%)	25.68 (99.4)	23.33 (99.3)
max./min. transm.	0.9262/0.8366	0.9455/0.9369
data/params	9520/595	7466/568
goodness-of-fit on F <sup>2</sup>	1.046	0.835
final R indices	R <sub>1</sub> = 0.0446	R <sub>1</sub> = 0.0387
[I > 2σ(I)]	wR <sub>2</sub> = 0.0923	wR <sub>2</sub> = 0.1328
R indices (all data)	R <sub>1</sub> = 0.0978	R <sub>1</sub> = 0.0402
	wR <sub>2</sub> = 0.1139	wR <sub>2</sub> = 0.1694
largest dif. peak/hole	1.004/−1.016	0.735/−0.609

**Table 2.** Selected bond lengths and angles for compounds **2** and **4**

	<b>2</b>	<b>4</b>
Distances (Å)		
Ag(1)–P(1)	2.4170(15)	Ag(1)–P(1) 2.4255(11)
Ag(1)–S(1)	2.6366(14)	Ag(1)–S(1) 2.5888(12)
Ag(1)–S(2) <sup>a</sup>	2.4537(14)	Ag(1)–S(2) 2.4956(12)
Ag(1)–N(11)	2.707(4)	Ag(1)–N(11) 2.675(4)
Ag(2)–P(2)	2.4360(4)	Ag(2)–P(2) 2.4454(11)
Ag(2)–S(1)	2.5609(14)	Ag(2)–S(1) <sup>b</sup> 2.5178(10)
Ag(2)–S(2)	2.4991(13)	Ag(2)–S(2) 2.5807(12)
Ag(2)–N(21)	2.754(4)	Ag(2)–N(21) 2.781(4)
Ag(1)–Ag(1) <sup>a</sup>	4.9810(9)	Ag(1)–Ag(1) <sup>a</sup> 4.4923(7)
Ag(1)–Ag(2)	4.7614(8)	Ag(1)–Ag(2) <sup>b</sup> 3.3966(5)
Ag(1)–Ag(2) <sup>a</sup>	3.3289(6)	Ag(1)–Ag(2) <sup>b</sup> 4.2977(6)
Ag(2)–Ag(2) <sup>a</sup>	6.5342(11)	Ag(2)–Ag(2) <sup>b</sup> 6.3114(8)
S(1)–S(1)	3.544(3)	S(1)–S(1) <sup>b</sup> 3.966(2)
S(1)–S(2)	4.2066(18)	S(1)–S(2) <sup>b</sup> 4.2197(3)
S(2)–S(2)	7.546(3)	S(2)–S(2) <sup>b</sup> 7.517(3)
S(1)–C(18)	1.722(6)	S(1)–C(18) 1.716(5)
S(2)–C(28)	1.781(5)	S(2)–C(28) 1.775(5)
Angles (deg)		
P(1)–Ag(1)–S(1)	110.70(5)	116.39(4) P(1)–Ag(1)–S(1)
P(1)–Ag(1)–S(2) <sup>a</sup>	140.49(5)	131.40(5) P(1)–Ag(1)–S(2)
P(2)–Ag(2)–S(1)	121.14(5)	128.37(4) P(2)–Ag(2)–S(1) <sup>b</sup>
P(2)–Ag(2)–S(2)	126.26(5)	115.98(4) P(2)–Ag(2)–S(2)
S(1)–Ag(1)–S(2) <sup>a</sup>	108.40(5)	112.17(4) S(1)–Ag(1)–S(2)
S(1)–Ag(2)–S(2)	112.47(4)	114.14(4) S(1) <sup>b</sup> –Ag(2)–S(2)
Ag(1)–S(1)–Ag(2)	132.72(6)	114.61(4) Ag(1)–S(1)–Ag(2)
Ag(1) <sup>a</sup> –S(2)–Ag(2)	84.46(4)	83.98(4) Ag(1)–S(2)–Ag(2)

<sup>a</sup>Symmetry transformations:  $-x + 1, -y + 1, -z + 1$ . <sup>b</sup> $-x, -y + 1, -z + 1$ .

rise to the crystalline compound [Ag<sub>2</sub>(LPEt)(HLPEt)]<sub>2</sub>(NO<sub>3</sub>)<sub>2</sub>·2MeOH·2H<sub>2</sub>O (**4**). On this occasion, as expected, compounds **3** and **4** have similar formulations, the

(15) APEX2, v.2.0-1; Bruker AXS Inc.: Madison, WI, 2005.

(16) Sheldrick G. M. *SADABS*; University of Gottingen: Gottingen, Germany, 1997.

(17) Sheldrick, G. M. *Acta Crystallogr.* **2008**, *A64*, 112–122.

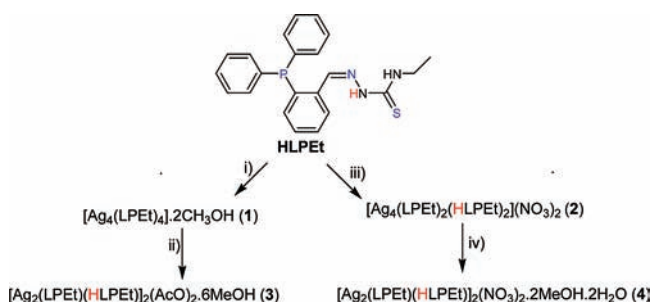
(18) Brandenburg, K. *DIAMOND*, version 3.1f; Crystal Impact GbR: Bonn, Germany, 2008.

**Table 3.** Hydrogen Bond Parameters [Å, deg] for Clusters **2** and **4**

D—H...A	D—H	H...A	D...A	∠DHA
<b>2<sup>a</sup></b>				
N(12)—H(12A)...O(11)	0.97	1.79	2.738(6)	164.7
N(13)—H(13A)...O(12)	0.90	1.98	2.785(6)	148.8
N(23)—H(23A)...O(4) <sup>a</sup>	0.99	1.90	2.824(6)	153.6
O(3)—H(3)...N(22) <sup>b</sup>	0.88	2.05	2.929(6)	173.7
O(4)—H(4)...O(12)	0.99	1.82	2.682(6)	143.4
O(5)—H(5)...O(11)	1.01	1.72	2.710(6)	166.7
<b>4<sup>b</sup></b>				
N(12)—H(12A)...O(11) <sup>b</sup>	0.89	2.19	2.857(5)	131.6
N(12)—H(12A)...O(13) <sup>a</sup>	0.89	2.42	3.104(5)	134.2
N(13)—H(13A)...O(13) <sup>b</sup>	0.85	2.01	2.851(5)	170.5
O(1)—H(1)—O(11)	0.82	2.16	2.792(5)	133.8
O(2)—H(2A)—O(1) <sup>c</sup>	0.95	2.21	2.829(5)	122.1
O(2)—H(2B)—O(2) <sup>d</sup>	0.96	2.18	2.873(6)	128.4

<sup>a</sup> Symmetry transformations for **2**: a:  $x - 1, y, z$ ; b:  $x, y, z + 1$ .

<sup>b</sup> Symmetry transformations for **4**: a:  $-x, -y + 1, -z + 1$ ; b:  $x - 1, y, z$ ; c:  $-x + 1, -y + 1, -z + 1$ ; d:  $-x + 1, -y, -z + 1$ .

**Scheme 1<sup>a</sup>**

<sup>a</sup> (i) AgOAc, MeOH; (ii) RT, MeOH; (iii) AgNO<sub>3</sub>, MeOH; (iv) RT, MeOH.

incorporation of a water molecule being the only change having occurred during the crystallization process.

The four compounds are air-, light-, and moisture-stable solids (**1** and **3**) or crystals (**2** and **4**) at room temperature. They were readily characterized by elemental analysis, mass spectrometry, and IR and NMR spectroscopy (<sup>1</sup>H and <sup>31</sup>P).

The appearance of the [M<sub>4</sub>(H<sub>x</sub>L)<sub>4</sub> + H]<sup>+</sup> peak in the MS-ESI<sup>+</sup> spectra of complexes **1** and **2** confirms the proposed tetranuclear stoichiometries. For the cationic compounds **3** and **4**, despite the fact that the higher peaks identified by MS-ESI<sup>+</sup> were [Ag<sub>3</sub>(H<sub>x</sub>L)<sub>3</sub> + H] (in these two cases additional MALDI experiments were unsuccessful), we are confident of their tetranuclear nature, because a similar fragmentation pattern was observed before for other thiosemicarbazone cluster complexes,<sup>14</sup> probably being evidence of the coexistence of different nuclearity species in solution. This fact is further indicated by the splitting of the amine and the imine signals in the <sup>1</sup>H NMR of the nitrate complexes.

Molar conductivity measurements performed for complex **1** suggest a nonelectrolytic character for this compound, although the relatively high value could be indicative of the existence of equilibria with 1:1 electrolyte species. However, the conductivity values found for complexes **2–4** are totally in accordance with 1:1 types of electrolytes.<sup>19</sup> These conclusions are also supported by the presence of the typical bands corresponding to acetate

or nitrate counterions in the IR spectra of complexes **2–4**. In addition, the disappearance of the NH amine proton in the <sup>1</sup>H NMR spectrum of complex **1** is in agreement with the deprotonation of the four ligands in this complex. On the contrary, the <sup>1</sup>H NMR spectra of compounds **2–4** display the amine NH signals slightly shifted downfield, as a consequence of the silver coordination. The imine signals exhibit a significant displacement in all of the compounds, which could indicate that the clusters' formation involves some interaction with the imine nitrogen donor atoms. The coordination of the phosphorus atoms in all of the complexes was confirmed in the displacement experiment by the <sup>31</sup>P resonance to positive values in the spectrum of the four complexes. This downfield shift is smaller for the neutral complex **1** than for the cationic analogues **2–4**, which indicates that the <sup>31</sup>P signal can be influenced by the charge of the compound. Moreover, the <sup>31</sup>P NMR of the nitrate complex **4** displays two overlapped peaks, which indicates the existence of two phosphorus atoms located in similar coordinative environments.

**X-Ray Determinations of Complexes 2 and 4.** The X-ray analysis revealed that complexes **2** and **4** consist of discrete cationic tetranuclear silver complexes, featuring Ag<sub>4</sub>S<sub>4</sub> metallacycle frameworks through a crystallographic inversion center (Figure 1). In every complex, four ligand molecules, two neutral and two anionic, are coordinated to four silver anions through a bidentate [PS] kernel. Additionally, the structure of **2** contains two acetate counterions and six solvating methanol molecules, while the structure of **4** displays two nitrate groups to balance the charge, being solvated by two methanol and two water molecules. It is important to note here the fact that both crystals **2** and **4** correspond to similar cationic clusters, which seems to point to the cationic tetranuclear aggregate as the most stable structure in the solid state, regardless of the metal precursor employed.

Every silver atom is coordinated to the thioamide sulfur and the phosphorus atoms of one ligand thread and a sulfur donor belonging to a second ligand unit, assuming a [PS<sub>2</sub>] distorted planar-trigonal environment. The distortion from the proposed geometry is indicated in both structures by the P—Ag—S bond angles, in the range 110–140°, and could be attributed to the long bite of the ligand, which is bound to the metal using the P,S-side donor atoms, the central imine nitrogen atoms remaining uncoordinated (see P—S distances in Figures 1 and 2).

Each silver atom is μ<sub>2</sub>-bridged by the sulfur atoms belonging to two different ligands to give rise to eight-membered metallarings having 'twist-chair' (**2**) or 'chair' (**4**) conformations (Table S1, Supporting Information),<sup>20</sup> as shown in Figure 2. In these rings, the silver–silver distances [Ag(1)—Ag(2)<sup>a</sup> 3.3289(6) Å in **2** (a: 1 - x, 1 - y, 1 - z) and Ag(1)—Ag(2) 3.3966(5) Å in **4**] are, although longer than in metallic silver [2.889(6) Å],<sup>21</sup> shorter than twice the van der Waals radius of this metal

(20) Pérez, J.; García, L.; Carrascosa, R.; Pérez, E.; Serrano, J. L. *Polyhedron* **2008**, *27*, 2487–2493.

(21) Wells, A. F. *Structural Inorganic Chemistry*, 5th ed.; Clarendon Press: London, 1990; p 1015.

(19) Geary, W. J. *Coord. Chem. Rev.* **1971**, *7*, 81–122.

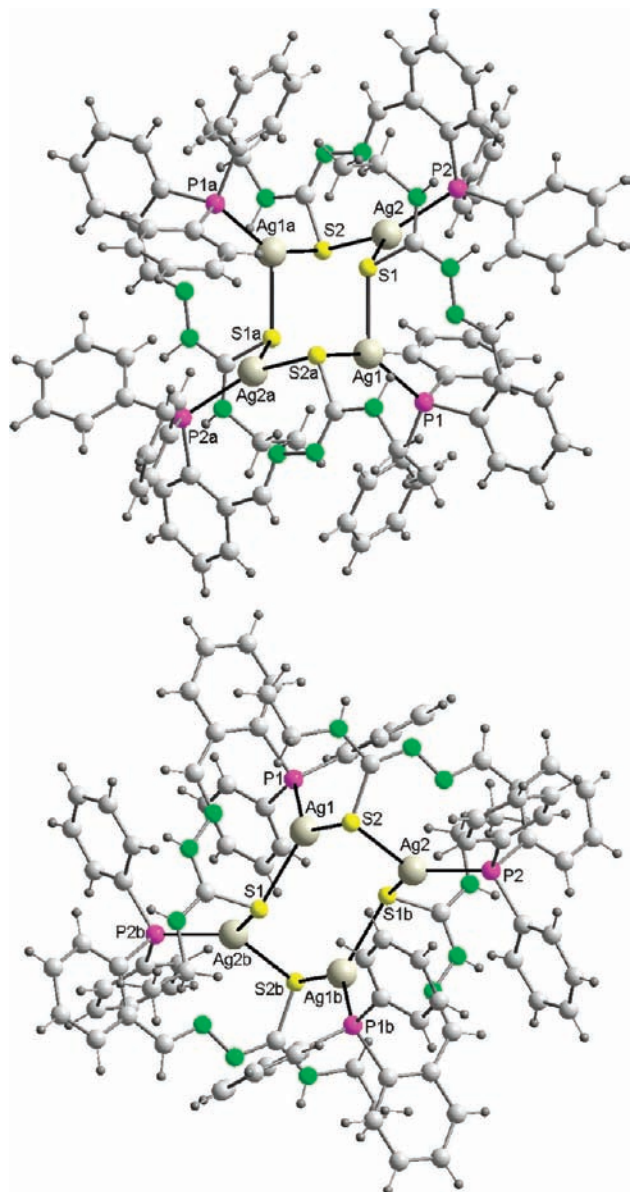


**Figure 1.** Representation of clusters  $[\text{Ag}_2(\text{LPEt})(\text{HLPEt})]_2^{2+}$  (**2**) (top) and  $[\text{Ag}_2(\text{LPEt})(\text{HLPEt})]_2^{2+}$  (**4**) (bottom) with labeling scheme for silver, sulfur, and phosphorus atoms. Atoms marked with the letter “a” are at the symmetry position  $(1-x, 1-y, 1-z)$  for **2**. Atoms marked with the letter “b” are at the symmetry position  $(-x, 1-y, 1-z)$  for **4**.

(3.44 Å),<sup>22</sup> and in light of previous works,<sup>11–14</sup> this suggests the existence of significant Ag–Ag interactions. Nevertheless, the distances between opposite metal atoms  $[\text{Ag}(1)–\text{Ag}(1)^a = 4.9810(9)$  Å and  $\text{Ag}(2)–\text{Ag}(2)^a = 6.5342(11)$  Å in **2**;  $\text{Ag}(1)–\text{Ag}(1)^b = 4.4923(7)$  Å and  $\text{Ag}(2)–\text{Ag}(2)^b = 6.3114(8)$  Å ( $b: -x, 1-y, 1-z$ ) in **4**] are indicative of an interaction not being established through the metallacycle. In addition, the Ag–S bond distances are as one would expect,<sup>23</sup> with the bridges being essentially symmetric, but showing different patterns in the two clusters. The central Ag–S bond distances are longer in the acetate cluster **2** [ $\text{Ag}(1)–\text{S}(1)$  and  $\text{Ag}(2)–\text{S}(1)$ ] than in the nitrate cluster **4** [ $\text{Ag}(1)–\text{S}(1)$  and  $\text{Ag}(2)–\text{S}(1)^b$ ]. On the contrary, the external Ag–S distances  $[\text{Ag}(1)–\text{S}(2)^a$

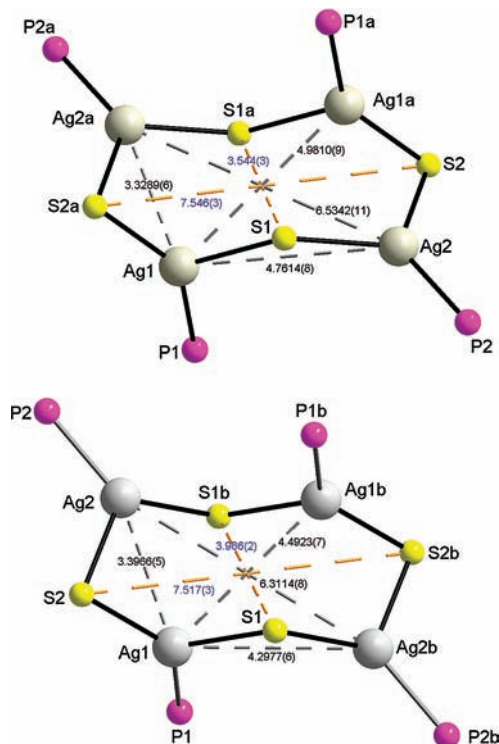


**Figure 2.** Perspective representations of the  $\text{Ag}_4\text{S}_4\text{P}_4$  central cores of clusters **2** (top) and **4** (bottom), illustrating the  $\text{Ag}_4\text{S}_4$  metallacycle structures. Atoms marked with “a” are at the symmetry position  $(1-x, 1-y, 1-z)$  for **2**, and atoms marked with “b” are at the symmetry position  $(-x, 1-y, 1-z)$  for **4**.

and  $\text{Ag}(2)–\text{S}(2)$  in **2**,  $\text{Ag}(2)–\text{S}(2)$  and  $\text{Ag}(1)–\text{S}(2)$  in **4**] are longer in the nitrate cluster **4**. Moreover, the position adopted by the two opposite S1 atoms differs in the two aggregates, these atoms being closer in acetate cluster **2**. All of these geometrical parameters clearly indicate the different sizes of the  $\text{Ag}_4\text{S}_4$  metallacycles in the two clusters: cluster **2** has approximate dimensions of 7.546(3) Å long and 3.544(3) Å wide, while for cluster **4**, the dimensions are 7.517(3) Å long and 3.966(2) Å wide. Although the phosphorus atoms are not involved in the cycles, it is worthy to note that the particular orientation adopted by the P1 atoms is also different in the two aggregates, showing the different alternate conformations adopted by the chair structures. This case of deformational isomerism may be attributed to different crystal packing originated by the presence of different anions and solvent molecules in the crystal lattice, because the crystal packing energies in **2** and **4** are probably of similar magnitude to the distortion energies of the coordination stereochemistry.<sup>8</sup>

The  $\text{Ag}\cdots\text{N}$  bond distances in both complexes fall in the interval 2.675(4)–2.781(4) Å (Table 2), being significantly longer than the average value of 2.460 Å found for Ag(I) thiosemicarbazone derived complexes.<sup>11–14</sup> However, the  $\text{Ag}\cdots\text{N}$  distances in these two clusters are shorter than the van der Waals radii sum (3.25 Å),<sup>24</sup> which suggests the existence of some kind of a secondary interaction. The higher affinity of silver for a “softer”

(22) Bondi, A. J. *Phys. Chem.* **1964**, *68*, 441–451.

(23) Bürgi, H.-B.; Dunitz, J. D. *Structure Correlations*; VCH: Weinheim, Germany, 1994; Vol. 2.

(24) Huheey, J. E.; Keiter, E. A.; Keiter, R. L. *Inorganic Chemistry: Principles of Structure and Reactivity*, 4th ed.; Harper Collins: New York, 1993.

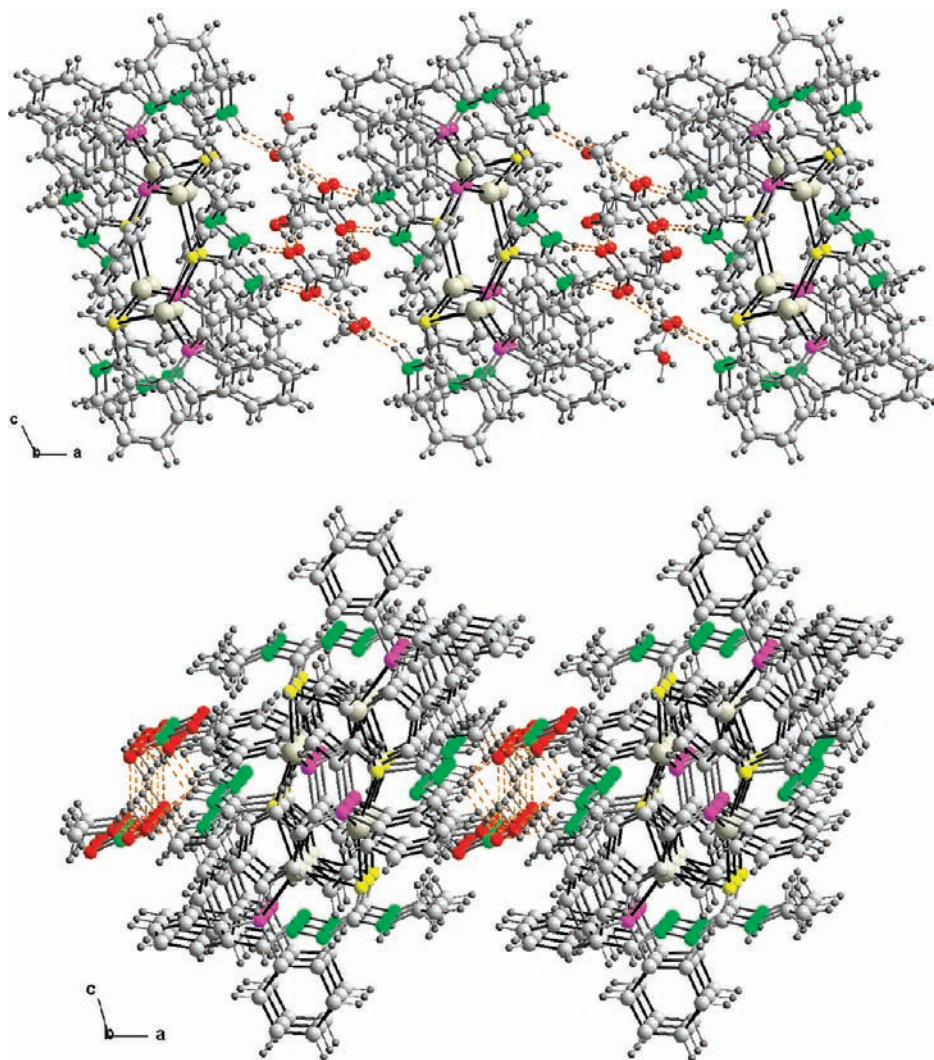


**Figure 3.** Partial packing diagram of **2** (up) and **4** (down) showing the lattice solvent molecules, the anions inserted between the clusters, and the formation of chains along “*a*” axis. Hydrogen bonds are distinguished by dashed orange lines (see also Figures S1 and S2, Supporting Information).

donor such as sulfur and the big size of the 4d metal may be two of the reasons explaining the preference of the silver atoms for a distorted planar-trigonal-geometry  $\text{AgS}_2\text{P}$  rather than for a distorted-tetrahedral-kernel  $\text{AgNS}_2\text{P}$ , which would be reached considering the mean contact  $\text{Ag}\cdots\text{N}$ .

In the crystal packing of both compounds, the cluster molecules are linked by hydrogen-bond interactions involving the thiosemicarbazone/thiosemicarbazionate donor atoms, the acetate (**2**) and nitrate (**4**) counterions, and the solvating molecules (Table 3). In both cases (**2** and **4**), the hydrogen-bonding pattern gives rise to cluster columns with anions and solvent molecules intercalated in the *a* axis direction (Figure 3). Such independent columns feature a 2D network in compound **2** (Figure S1a, Supporting Information) containing  $\text{Ag}_4\text{S}_4$  cyclooctane-type voids along the *b* axis (Figure S2a, Supporting Information). Another aspect to be considered is that cluster **4** assembles a 3D architecture (Figure S1b, Supporting Information), with the clusters connected by hydrogen bonds involving the water molecules ( $\text{O}_2$ ), but without any void in the structure (Figure S2b, Supporting Information). Nevertheless, the crystal packing of **2** is less compact because it exhibits voids around the

coordinates  $-0.008, 0.000, 0.000$  (Figure 4). This fact is numerically reflected by the “*total potential solvent area per unit cell*” value,  $459.7 \text{ \AA}^3$  in **4**, which corresponds to 17.7% empty volume, compared with the  $14.6 \text{ \AA}^3$  (0.6% empty volume) of cluster **2**.

It is also interesting to analyze whether the origin of the difference in the internal  $\text{Ag}_4\text{S}_4$  rings’ sizes arises from the counterion role in the crystal packing (two acetates in **2** and two nitrate groups in **4**). While the two nitrate oxygen atoms establish intermolecular hydrogen-bond interactions with the hydrazide and thioamide hydrogen atoms belonging to a neighboring thiosemicarbazone molecule in **4**, the acetate oxygen atoms are hydrogen-bonded to the same donors in cluster **2**, but belonging to the same asymmetric unit. This different hydrogen-bond pattern (Table 3) illustrates a more expanded metallamacrocycle structure and explains the bigger size of the cavity in the nitrate cluster **4** compared with that in the acetate cluster **2**.

A careful comparison of these two silver cluster compounds with the neutral cluster  $[\text{Ag}(\text{mtsc})]_4 \cdot 2\text{CHCl}_3$ , synthesized by Nomiya et al.,<sup>14</sup> also displaying a  $\text{Ag}_4\text{S}_4$  internal cycle, lets us remark on notable differences between them: our clusters **2** and **4** show the silver

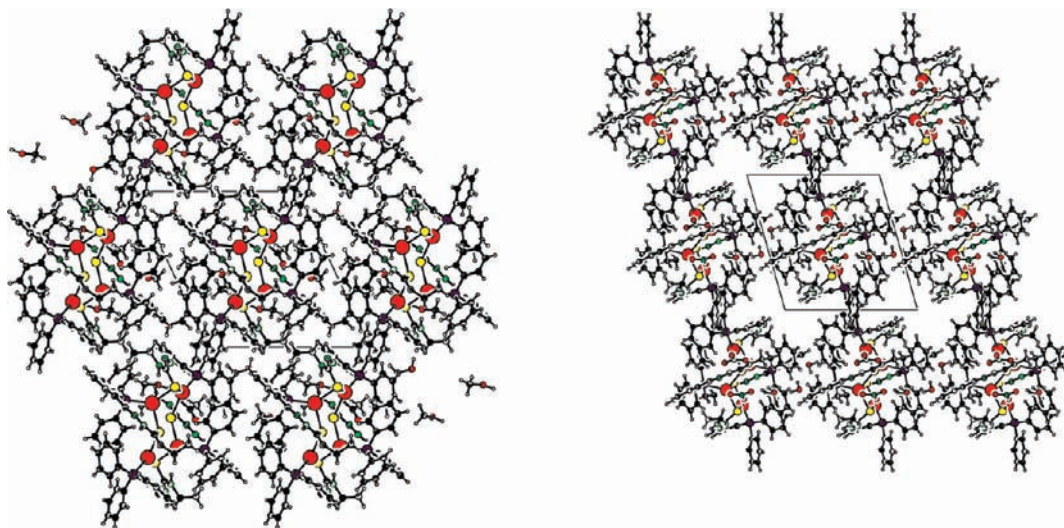


**Figure 4.** Cell diagram for the crystal structures of **2** (left) and **4** (right) projected in the *bc* plane.

in a distorted planar-trigonal environment, the imine nitrogen remaining unbound in the four ligand threads, whereas in the Nomiya core, the silver atoms are four-coordinated by the three donor atoms of the thiosemicarbazone ligand. As a consequence of this, the  $\text{Ag}_4\text{S}_4$  ring is more expanded in **2** and **4** because the silver metal ions are bound to the donors located in the extremes of the thiosemicarbazone skeleton, which results in a longer coordination bite and therefore in a bigger size of the internal rings. The bigger size of the cavity in our clusters is also demonstrated by the fact that argentophilic interactions do not exist between opposite silver centers in the central metallaring [ $\text{Ag}(1)-\text{Ag}(1)^a = 4.9810(9)$  Å in **2** and  $\text{Ag}(1)-\text{Ag}(1)^b = 4.4923(7)$  Å in **4**], while significant interactions are present in  $[\text{Ag}(\text{mtsc})_4 \cdot 2\text{CHCl}_3]$  [ $\text{Ag}2-\text{Ag}2^i = 3.2111(11)$  Å]. Moreover, and in contrast with the Nomiya clusters, which could be fragmented into dimers by reaction with triphenylphosphine, our clusters **2** and **4** have turned out to be more robust, because their reaction with triphenylphosphine (molar ratio 1:4) yielded a solid which was identified as a mixture of the starting materials (these results were further confirmed after  $^{31}\text{P}$  NMR titrations of **3** and **4** with  $\text{PPh}_3$ ). For that reason, phosphino thiosemicarbazone ligands are revealed as highly suitable skeletons for the assembly of thiosemicarbazone silver clusters.

**Checking the Factors Involved in the Assembly of Thiosemicarbazone Silver Clusters.** In our previous work analyzing the factors involved in the assembly of  $\text{Ag}(I)$  clusters with thiosemicarbazones, we remarked on some aspects involved in the formation of these types of compounds.<sup>12</sup> At this time, and in the light of the two new structures presented in this work, some of the factors previously established for the assembly of silver thiosemicarbazone aggregates must be revised. One of these aspects is related with the deprotonation degree of the thiosemicarbazone ligand, because all of the previous examples clearly indicated that all of the ligand units involved in the assembly of a thiosemicarbazone cluster must be deprotonated.<sup>12–14</sup> It is particularly noteworthy that this basic principle is broken by the two new structures herein reported, which contain two of the four

ligands undeprotonated, generating to the best of our knowledge the first two cases of cationic thiosemicarbazone silver clusters, because the previous examples are neutral cluster molecules. In addition, the reported cluster examples indicated that the use of two of the three donor atoms in all of the tridentate thiosemicarbazone ligands involved in the cluster gave rise to hexanuclear species, whereas if the three donor atoms were coordinated in at least two ligand units, the aggregate formed turned out to be tetranuclear.<sup>12–14</sup> These trends are also broken by compounds **2** and **4**, as they were assembled by using only two of the donor atoms of every ligand strand, with the imine or the hydrazide nitrogen atoms remaining unbound. As a consequence of this fact, these two  $\text{Ag}_4\text{S}_4\text{P}_4$  core structures were formed by using only eight donor atoms, two donors less than our previously reported  $\text{Ag}_4\text{N}_2\text{S}_4\text{P}_4$  clusters  $[\text{Ag}_4(\text{LPPH})_4]^a[\text{Ag}_4(\text{LPPH})_4]^b \cdot 8\text{MeOH}$ ,<sup>12</sup> or the 12 donors involved in the  $\text{Ag}_4\text{N}_8\text{S}_4$  Nomiya cluster  $[\text{Ag}(\text{mtsc})_4] \cdot 2\text{CHCl}_3$ .<sup>14</sup> The existence of four imine donors unbound leads us to think that the nuclearity of these clusters may be increased by use of suitable metal scaffolds. Another new factor to highlight is that the change of a phenyl group to a less bulky ethyl group in the thioamide nitrogen atom of the thiosemicarbazone does not modify the nuclearity of the cluster formed (four), but it notably affects the cluster microarchitecture.<sup>12</sup> Thus, the two cluster structures reported herein constitute unique examples of cationic thiosemicarbazone silver clusters, as they exhibit unprecedented core arrangements.

**Luminescence Studies.** Inorganic–organic hybrid coordination compounds have been investigated for fluorescent properties and for potential applications as luminescent materials, such as light-emitting diodes,<sup>25</sup> because of their ability to affect the emission wavelength and strength of organic materials. The judicious choice of suitable conjugated organic skeletons and transition-metal centers can be an efficient method for obtaining

(25) Wang, Q.-M.; Lee, Y.-A.; Crespo, O.; Deaton, J.; Tang, C.; Gysling, H. J.; Gimeno, M. C.; Larraz, C.; Villacampa, M. D.; Laguna, A.; Eisenberg, R. *J. Am. Chem. Soc.* **2004**, *126*, 9488–9489. Evans, R. C.; Douglas, P.; Winscom, C. J. *Coord. Chem. Rev.* **2006**, *250*, 2093–2126.

new types of photoluminescent materials, especially for  $d^{10}$  or  $d^{10}-d^{10}$  systems.<sup>26</sup> It is well-known that the presence of direct metal–metal interactions may be one of the important factors contributing to the luminescent properties of  $d^{10}$  metal compounds. This finding is perfectly exemplified by the large number of reported polynuclear silver complexes which exhibit luminescence.<sup>27</sup> Nevertheless, until now, only a few of these Ag(I) complexes have been reported to be emissive at room temperature,<sup>28</sup> since most of them only exhibit emission at low temperatures.<sup>29</sup> Particularly in the field of silver thiosemicarbazone complexes, the number of luminescence studies is very limited,<sup>30</sup> which makes difficult at the present moment a determination of the exact origin of the emission displayed by Ag(I) thiosemicarbazone clusters. With the aim of contributing more data and bringing more light to this area, we have measured the luminescence properties of the ligand HLPet and its cluster-derived M(I) complexes **1**–**4**. Having in mind the different stoichiometry of the neutral solid **1** and the crystalline cluster **2**, both obtained from the same reaction, together with the same cationic charge of nitrate clusters **3** and **4**, we also expect to assess whether the charge and the counterion nature have any influence on the luminescent properties of these cluster compounds.

All of the emission spectra for the ligand and the complexes are shown in Figure 5. The ligand HLPet and silver complexes **1**–**4** are strongly luminescent at room temperature, in methanol solutions. In the emission spectrum of HLPet, a broad band at 420 nm and a shoulder at 540 nm were observed when they were excited at 325 nm. The tetranuclear complex **1** also shows two emission bands centered at 425 and 508 nm upon excitation at 350 nm. The main emission wavelength of **1** (425 nm) is quite similar to that displayed for a related tetranuclear silver cluster derived from a related phosphino thiosemicarbazone ligand  $[\text{Ag}(\text{LPPH})_4] \cdot 2\text{MeOH}$  (436 nm), previously reported by us.<sup>12</sup> Moreover, complex **2**, obtained by crystallization of the mother liquors, emits blue fluorescence as a single band at 470 nm upon excitation at the same wavelength (350 nm). This different emission pattern is in accordance with the neutral and cationic character of **1** and **2**, respectively, and demonstrates that the nature of the emission is influenced by the charge of the complexes. As expected, because of their similar nature, the nitrate complexes **3** and **4** display similar violet luminescence with bands at 390 nm upon excitation at 360 nm in their spectra, broad for the solid **3** and sharp for the crystalline compound **4**. In addition, the existence of a multiple-band emission for these complexes

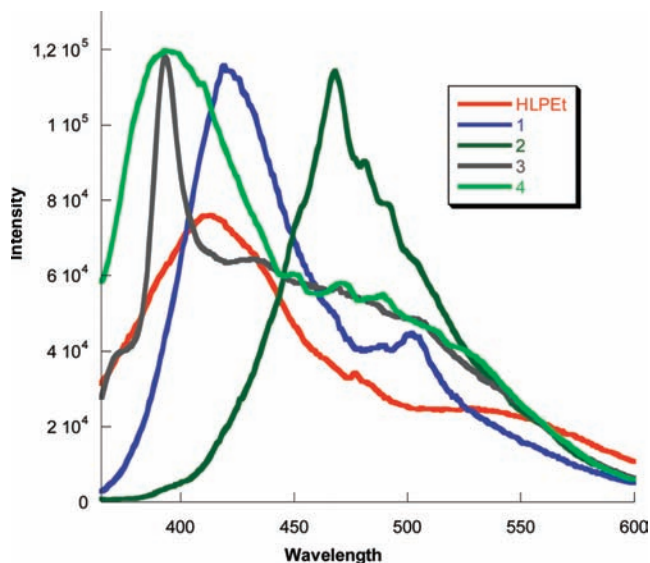


**Figure 5.** Emission spectra of the ligand HLPet and the complexes **1**–**4** in methanol ( $1 \times 10^{-5}$  M).

could suggest the presence of different weakly coupled relaxation channels in this complex, as was found in other compounds containing closed-shell  $d^{10}$  metal centers.<sup>31</sup> From the obtained results, it is clear that the nature of the counterion (acetate for **2** and nitrate for **4**) modifies the wavelength of the emission, being red-shifted in the case of the nitrate-derived clusters. However, an increasing of the anion concentration in the media modifies neither the emission wavelength nor the intensity.

Another aspect to highlight is that the emission of the ligand HLPet is shifted and notably enhanced by the coordination of the silver ions to the ligands. This enhancement can be ascribed to the silver cluster-based centers therein,<sup>27</sup> although other factors like the increasing of the conformational rigidity and conjugation of the charge in the ligand skeleton could also contribute.<sup>32</sup>

The origin of luminescence for  $d^{10}$  metal clusters seems to be highly dependent on the particular metal core features shown in the solid state.<sup>33</sup> In the absence of luminescence data for similar clusters containing  $\text{Ag}_4\text{S}_4$  metallamacrocycles, and having in mind the square-planar geometry adopted by the silver atoms in clusters **2** and **4**, as well as their halide-free nature, we dare to assign their emissions to ligand-to-metal charge transfer transitions, although a mixed nature, with the contribution of a metal-centered (MC, d-s or d-p) state, could also be probable.<sup>31,33,34</sup>

(26) Ciurtin, D. M.; Pschirer, N. G.; Smith, M. D.; Bunz, U. H. F.; Loye, H.-C. Z. *Chem. Mater.* **2001**, *13*, 2743–2745. Cariati, E.; Bu, X.; Ford, P. C. *Chem. Mater.* **2000**, *12*, 3385–3391. Harvey, P. D.; Gray, H. B. *J. Am. Chem. Soc.* **1988**, *110*, 2145–2147. Seward, C.; Jia, W.-L.; Wang, R.-Y.; Enright, G. D.; Wang, S.-N. *Angew. Chem., Int. Ed.* **2004**, *43*, 2933–2936. Ding, B.; Yi, L.; Wang, Y.; Cheng, P.; Liao, D. Z.; Yan, S. P.; Jiang, Z. H. *Dalton Trans.* **2006**, 665–675.

(27) Yang, J.; Zheng, S.; Yu, X.; Chen, X. *Cryst. Growth Des.* **2004**, *4*, 831–836 and references therein.

(28) Wei, Y.; Wu, K.; Zhuang, B.; Zhou, Z.; Zhang, M.; Liu, C. Z. *Anorg. Allg. Chem.* **2005**, *631*, 1532–1535 and references therein.

(29) Tong, M. L.; Chen, X. M.; Ye, B. H.; Ji, L. N. *Angew. Chem., Int. Ed.* **1999**, *38*, 2237–2240.

(30) Zhou, Y.; Zhang, X.; Chen, W.; Qiu, H. *J. Organomet. Chem.* **2008**, *693*, 205–215.

(31) Omary, M. A.; Rawashdeh-Omary, M. A.; Diyabalanage, H. V. K.; Dias, H. V. R. *Inorg. Chem.* **2003**, *42*, 8612–8614. Castiñeiras, A.; Garcia-Santos, I.; Dehnen, S.; Sevillano, P. *Polyhedron* **2006**, *25*, 3653–3660. Sevillano, P.; Fuhr, O.; Kattannek, M.; Nava, P.; Hampe, O.; Lebedkin, S.; Ahlrichs, R.; Fenske, D.; Kappes, M. M. *Angew. Chem., Int. Ed.* **2006**, *45*, 3702–3708. Zhou, Y.; Chen, W.; Wang, D. *Dalton Trans.* **2008**, 1444–1453. (32) Haasnoot, J. G. *Coord. Chem. Rev.* **2000**, *131*, 200–202.

(33) Catalano, V. J.; Kar, H. M.; Garnas, J. *Angew. Chem., Int. Ed.* **1999**, *38*, 1979–1982. Sevillano, P.; Fuhr, O.; Kattannek, M.; Nava, P.; Hampe, O.; Lebedkin, S.; Ahlrichs, R.; Fenske, D.; Kappes, M. M. *Angew. Chem., Int. Ed.* **2006**, *118*, 3785–3791.

(34) Crespo, O.; Gimeno, M. C.; Laguna, A.; Larraz, C.; Villacampa, M. D. *Chem.—Eur. J.* **2007**, *13*, 235–246. Zhou, Y.; Zhang, X.; Chen, W.; Qiu, H. *J. Organomet. Chem.* **2008**, *693*, 205–215.



### Concluding Remarks

In summary, the introduction of a phosphorus atom in a thiosemicarbazone ligand constitutes an appropriate approach which enables us to prepare two novel cationic thiosemicarbazone silver clusters featuring different-sized  $\text{Ag}_4\text{S}_4$  metallacycles. The size of the internal rings is determined by the nature of the anion neutralizing the cationic tetranuclear cluster, which also is responsible, together with the solvent molecules, for the different types of packing exhibited by the two clusters. We can also conclude that a cluster structure can be formed even if some of the participating thiosemicarbazone ligands stay as neutral molecules. Besides, the number of the donor atoms per ligand involved in the coordination to the silver centers

clearly influences the internal architecture of the core in the clusters formed. The four reported silver complexes are probed to be strongly fluorescent, the emission being determined by the charge of the compound and the nature of the counterion.

**Acknowledgment.** Financial support from Xunta de Galicia (INCITE08PXIB203128PR) is acknowledged. R.P. thanks Xunta de Galicia for an “Isidro Parga Pondal” contract.

**Supporting Information Available:** Figures S1 and S2, Table S1, CIF files for complexes **2** and **4**. This material is available free of charge via the Internet at <http://pubs.acs.org>.